JCB Article

Phospholipase C and cofilin are required for carcinoma cell directionality in response to EGF stimulation

Ghassan Mouneimne,[1] Lilian Soon,[1] Vera DesMarais,[1] Mazen Sidani,[1] Xiaoyan Song,[1] Shu-Chin Yip,[1,2] Mousumi Ghosh,[1] Robert Eddy,[1] Jonathan M. Backer,[2] and John Condeelis[1]

[1]Department of Anatomy and Structural Biology and [2]Department of Molecular Pharmacology, Albert Einstein College of Medicine, Bronx, NY 10461

The epidermal growth factor (EGF)–induced increase in free barbed ends, resulting in actin polymerization at the leading edge of the lamellipodium in carcinoma cells, occurs as two transients: an early one at 1 min and a late one at 3 min. Our results reveal that phospholipase (PLC) is required for triggering the early barbed end transient. Phosphoinositide-3 kinase selectively regulates the late barbed end transient. Inhibition of PLC inhibits cofilin activity in cells during the early transient, delays the initiation of protrusions, and inhibits the ability of cells to sense a gradient of EGF. Suppression of cofilin, using either small interfering RNA silencing or function-blocking antibodies, selectively inhibits the early transient. Therefore, our results demonstrate that the early PLC and cofilin-dependent barbed end transient is required for the initiation of protrusions and is involved in setting the direction of cell movement in response to EGF.

Introduction

Chemotaxis is a significant event central to many physiological and pathological processes. The motility cycle (Abercrombie et al., 1972) is elementary to chemotaxis in most organisms (Bailly and Condeelis, 2002), hence the similarity among the different models depicting this process. In fact, much evidence about chemotaxis has emerged from work on chemotactic ameboid cells such as neutrophils and *Dictyostelium discoideum*.

Studies on the cAMP-driven chemotaxis in aggregation competent *D. discoideum* ameoba demonstrated that cAMP induces a biphasic actin polymerization response in the cells. After stimulation with cAMP, actin polymerization peaks as early as 5 s, and this event is not associated with membrane protrusion, which begins later, around 30 s, when a second polymerization transient occurs (Hall et al., 1989; Cox et al., 1992; Eddy et al., 1997; Funamoto et al., 2002; Iijima and Devreotes, 2002; Chen et al., 2003). In carcinoma cells as well, EGF stimulation induces two actin polymerization transients (Chan et al., 1998, 2000). The importance of understanding how the location and timing of actin polymerization is regulated in carcinoma cells in response to EGF is that these cells are chemotactic to EGF in the primary tumor, and chemotaxis is directly correlated with metastasis (Wyckoff et al., 2000a,b).

The distinct functions of the two transients of actin polymerization in cell motility are not well understood. Moreover, little is known about the signaling pathways that regulate this biphasic actin response and about the relationships among them. The second transient of actin polymerization is phosphoinositide-3 kinase (PI3K) dependent in both *D. discoideum* and carcinoma cells (Hill et al., 2000; Chen et al., 2003). However, the signaling pathway that leads to the first actin polymerization transient is PI3K independent and is still unknown (Chen et al., 2003).

PI3K activity is believed to be an essential element in directional sensing of some cell types when placed in a shallow gradient of chemoattractant (Servant et al., 2000; Funamoto et al., 2002; Iijima and Devreotes, 2002). Directional sensing is defined as the detection of an asymmetric extracellular signal and the generation of an intracellular amplified asymmetric response (Chen et al., 2003; Devreotes and Janetopoulos, 2003). This amplification may be attained in *D. discoideum* by a reciprocal regulation of PI3K and PTEN activities, where PI3K is localized at the leading edge and PTEN at the sides and the rear of the migrating cell (Comer and Parent, 2002; Funamoto et al., 2002; Iijima and Devreotes, 2002).

Address correspondence to Ghassan Mouneimne, Dept. of Anatomy and Structural Biology, Albert Einstein College of Medicine, 1300 Morris Park Ave., Bronx, NY 10461. Tel: (718) 430-4113. Fax: (718) 430-8996. email: gmouneim@aecom.yu.edu

Key words: PLC; actin; PI3 kinase; motility; chemotaxis

Abbreviations used in this paper: PI3K, phosphoinositide-3 kinase; PIP2, phosphatidyl 4,5-biphosphate; siRNA, small interfering RNA.

The Journal of Cell Biology, Volume 166, Number 5, August 30, 2004 697–708
http://www.jcb.org/cgi/doi/10.1083/jcb.200405156

The Journal of Cell Biology

This asymmetrical distribution of the two antagonistic enzymes could lead to PIP3 accumulation at the leading edge and is proposed to trigger the signaling cascade that sustains the actin polymerization-dependent protrusive force.

Although there is much evidence supporting the idea that the direction of cell migration in *D. discoideum* is established and amplified by spatial control of PIP3 production and degradation, little is known about the upstream mechanisms that regulate the translocation and activation of PI3K and PTEN. That is, what sets the initial asymmetric localization of these enzymes in response to sensing of the chemoattractant? In mammalian cells, PTEN function is more implicated in cell cycle regulation, as a tumor suppressor, than it is in cell motility. PTEN loss of function is, in fact, correlated with the progression of several tumors and is a characteristic of many invasive cell lines (Wu et al., 2003). PTEN function has been recently shown to have an inhibitory effect on cell motility in mammalian cells (Raftopoulou et al., 2004). This finding implies that there is a distinct, PI3K-independent signaling mechanism in mammalian cancer cells for directional sensing.

In mammalian cells and *D. discoideum*, the sensing of the chemoattractant gradient is conveyed by growth factor and G-protein–coupled receptors, respectively. Interestingly, the spatial localization of the response, directed protrusion and motility, is not mirrored by a redistribution of the receptors to the leading edge (Funamoto et al., 2002; Iijima and Devreotes, 2002; Chen et al., 2003). Studies that addressed this concern about localization of the response demonstrated that, upon stimulation, a subpopulation of EGF receptors, with F-actin–binding activity (den Hartigh et al., 1992), directly interacts with the actin cytoskeleton. This fraction of receptors was shown to have higher affinity for EGF, possibly providing a hypersensitivity to the chemoattractant (Payrastre et al., 1991). This finding suggests that actin polymerization in association with EGF receptors could play a role in initiating the asymmetry in the sensing mechanism. An important contributor to this initial signaling cascade is PLC. Previous studies have shown that PLCγ is important for growth factor–mediated cell motility and for invasiveness of cancer cells (Falasca et al., 1998; Kassis et al., 2002). Moreover, the EGF receptor-associated PLCγ activity was demonstrated to be imperative for motility by itself, but not for mitogenesis (Chen et al., 1994).

The mechanism through which PLC remodels the actin cytoskeleton may be the activation of actin-binding proteins such as cofilin, gelsolin, and profilin (Goldschmidt-Clermont et al., 1991; Yonezawa et al., 1991; Sun et al., 1999; Allen, 2003). Cofilin, profilin, and gelsolin bound to phosphatidyl 4,5-biphosphate (PIP2) in an inhibited state in resting cells are postulated to be released upon PIP2 hydrolysis, leading to a localized remodeling of the actin cytoskeleton. Profilin supports subsequent actin polymerization by facilitating nucleotide exchange and biasing of actin monomers toward barbed end polymerization (dos Remedios et al., 2003). Gelsolin severing finishes by capping the barbed ends until membrane PIP2 levels are restored to cause uncapping of gelsolin (Sun et al., 1999). This is a relatively slow process with a half-life of 15 min after growth factor stimulation (Allen, 2003), inconsistent with a gelsolin contribution to the early EGF-dependent actin polymerization transient, which occurs in less than a minute (Chan et al., 2000). We have focused our efforts on the relationship between PLC and cofilin activity during the early transient.

In this work, we have determined the relative contributions of the PLC and PI3K pathways to the biphasic actin polymerization transients in carcinoma cells after EGF stimulation. We have studied the early transient in more detail because of its potential in setting the initial asymmetry during chemotactic stimulation. We identified cofilin as an essential downstream effector for actin polymerization during the early transient.

Results

EGF-induced actin polymerization follows two transients

In carcinoma cells, the EGF-induced actin polymerization activity is directly correlated with the generation of free barbed filament ends. EGF induces an increase in the number of free barbed ends in the nucleation zone (corresponding to the most peripheral 0.22 μm; Fig. 1 B, shaded area) of the leading edge, and this increase has two transients, with a major peak around 1 min after stimulation and a second smaller peak at 3 min (Fig. 1 C). These results were consistent with the previously determined high temporal resolution kinetic time course of barbed ends (Chan et al., 1998). In this work, we refer to the peak of barbed ends at 1 min as the early transient and to the peak of the barbed ends at 3 min as the late transient.

PLCγ activity is stimulated during the early barbed end transient

Previous studies indicated that PLCγ-dependent signaling pathways are important for cell motility (Kassis et al., 1999; Piccolo et al., 2002). This finding induced us to study the role of PLCγ in the EGF-induced free barbed end transients. We started by examining the activation of PLCγ in response to EGF stimulation. PLC activity is regulated by tyrosine phosphorylation (Rebecchi and Pentyala, 2000). Therefore, to measure the amount of activated PLC at several time points after EGF addition, we performed an immunoprecipitation using antiphosphotyrosine antibodies. The levels of PLC in the anti-P(Y) immunoprecipitates were then detected by Western blot using an anti-PLCγ1 antibody. The immunoblot band intensities were quantitated and standardized over the intensities of the corresponding IgG bands from the same blot (Fig. 2 A). These results show that PLCγ phosphorylation increases, by twofold, in response to EGF, peaks at 1 min, and drops to unstimulated levels by 2 min after stimulation. Treatment with U73122, a synthetic inhibitor drug specific for PLC (Bleasdale et al., 1989), suppresses the activity of PLC to basal levels (Fig. 2 C). Alternatively, anti-PLCγ [pY783] Western blotting was performed, and standardization over total PLCγ revealed that the levels of PLCγ [pY783] follow the same pattern observed by immunoprecipitation (Fig. 2 B). In both experiments, there was temporal concurrence between PLCγ activation and the early barbed end transient.

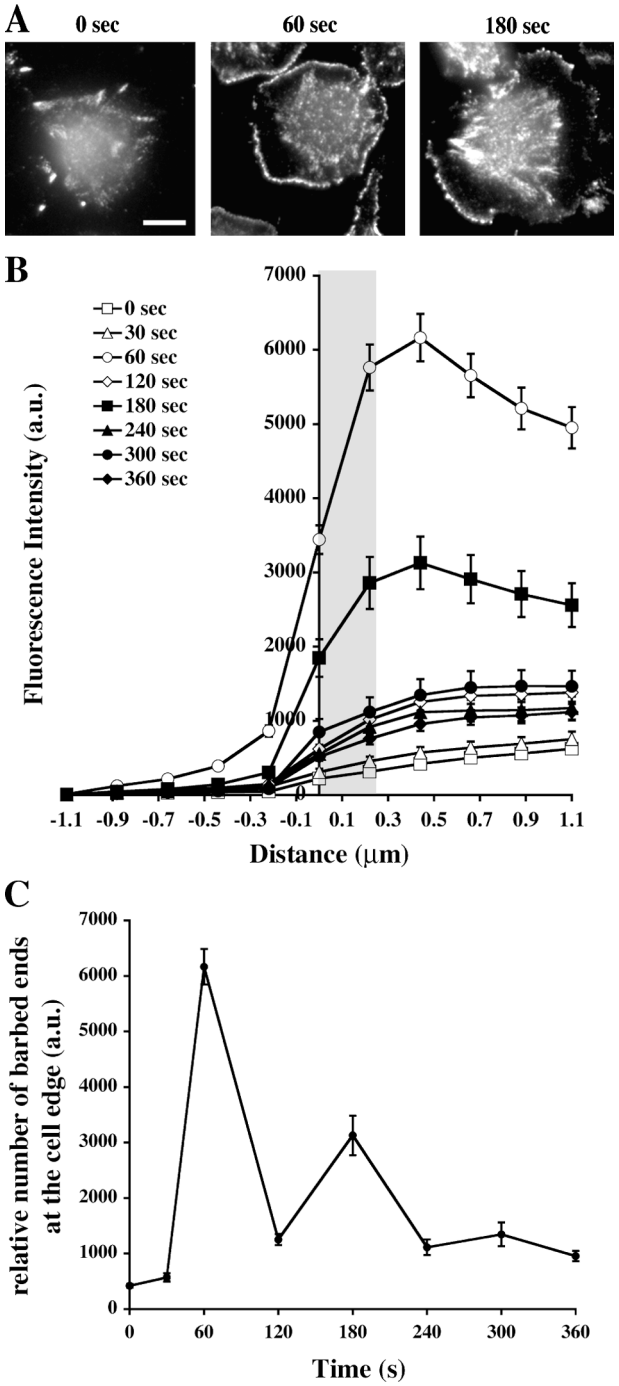

Figure 1. **The Barbed end assay, in MTLn3 cells, shows that EGF stimulation results in early and late barbed end transients at the leading edge.** (A) Representative images of EGF-stimulated cells (0, 60, and 180 s) with the barbed end staining at the leading edge. Bar, 10 μm. (B) The relative number of barbed ends (arbitrary units of fluorescence intensity) from 1.1 μm outside the cells (the membrane is at 0 μm) to 1.1 μm inside the cell periphery. (C) The relative number of barbed ends in the zone between 0 and 0.22 μm inside the cell edge (B, shaded area) versus time after addition of EGF. Error bars are SEM of ~60 cells, pooled from at least three independent experiments.

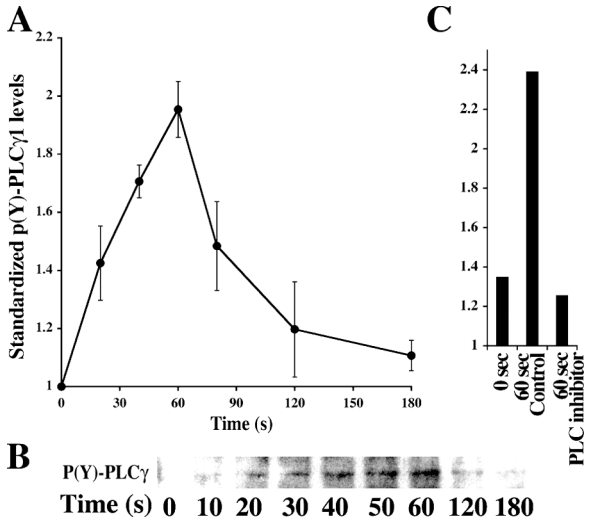

Figure 2. **PLCγ activity peaks at 60 s after EGF stimulation in MTLn3 cells.** (A) The plot of p(Y)-PLCγ levels, standardized over total IgG levels (from the same blot), versus time after EGF addition. Error bars are SEM of averages of three independent experiments. (B) Representative Western blot of PLCγ [pY783]. (C) Effect of the PLC inhibitor (U73122) as compared with control (the inactive isoform, U73343).

PLC inhibition selectively suppresses the generation of free barbed ends during the early transient

To determine the role of PLC in the EGF-induced generation of free barbed ends, we inhibited PLC activity with U73122 and measured the relative number of barbed ends after EGF addition using the barbed end assay (Fig. 3). U73343, the inactive isoform of the drug, and DMSO, the vehicle for both compounds, were applied as control treatments. Cells were treated for 10 min with U73122, U73343, or DMSO before EGF addition. Cells treated with U73122 showed a selective decrease in the barbed end edge staining during the early transient, as compared with DMSO (not depicted) and U73343 (Fig. 3 B). However, inhibition of PLC did not affect the barbed end staining during the late transient where the generation of free barbed ends still peaked at 3 min after EGF addition. These results showed that PLC inhibition selectively inhibits the generation of new barbed ends during the early barbed end transient but not the late transient. From this result, we concluded that the activation of PLC in response to EGF stimulation is a major regulator of the early transient. However, the inhibition of PLC did not have an obvious effect on the levels of total F-actin in resting cells, as were measured by rhodamine-phalloidin staining (Fig. 3 C). This result indicates that PLC inhibition is specifically suppressing actin polymerization during the early transient, and not through an indirect effect by inhibition of actin depolymerization.

PI3K inhibition selectively suppresses the generation of free barbed ends during the late transient

To reveal the involvement of PI3K in the EGF-induced generation of free barbed ends, we used wortmannin at a final concentration of 100 nM to specifically inhibit PI3K. Cells were treated for 15 min with wortmannin or with equal volume of DMSO or were left untreated (only switched to BSA-free medium; unpublished data). After the different treatments, the cells were analyzed using the barbed end assay, and the relative levels of barbed ends were quan-

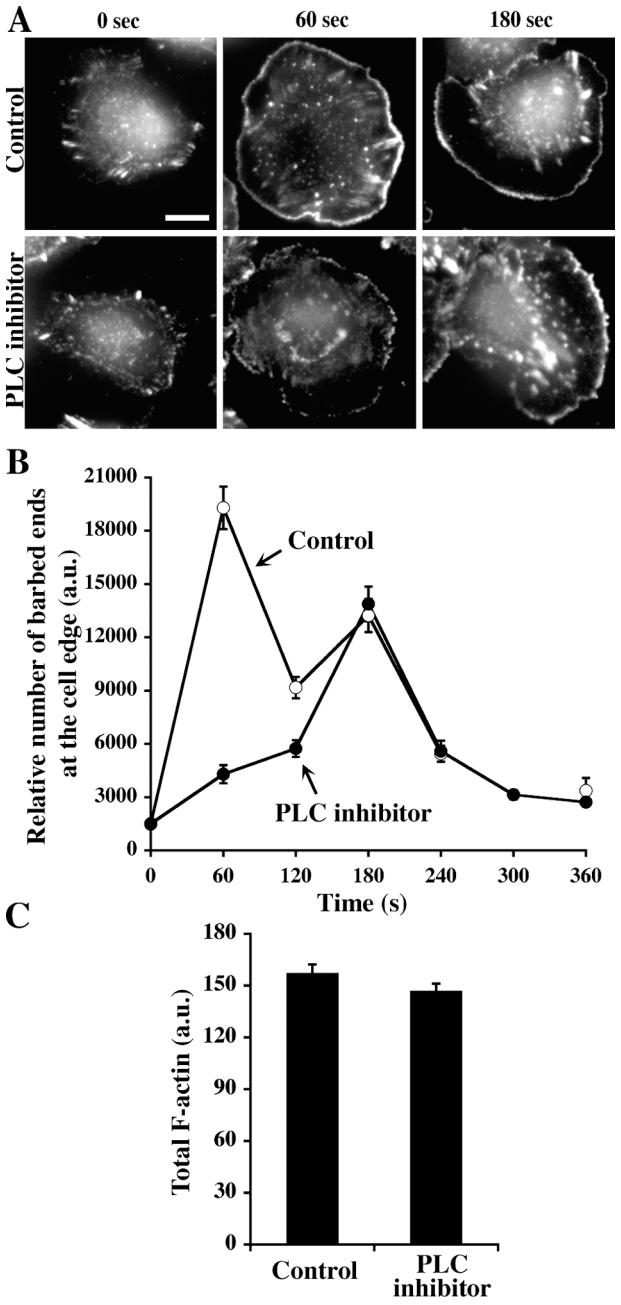

Figure 3. **PLC inhibition selectively suppresses the generation of free barbed ends during the early transient and not during the late transient without affecting the total levels of F-actin.** (A) Representative images of the barbed end assay of cells treated with the inactive isoform (control) or the PLC inhibitor at 0, 60, and 180 s after stimulation. Bar, 10 μm. (B) Plot of the relative number of barbed ends at 0–0.22 μm inside the cell versus time after stimulation in control (open circles) and PLC-inhibited (closed circles) MTLn3 cells. (C) Total F-actin levels in control and PLC-inhibited cells as measured by rhodamine-phalloidin staining. Error bars in both graphs are SEM of ~60 cells, pooled from at least three independent experiments.

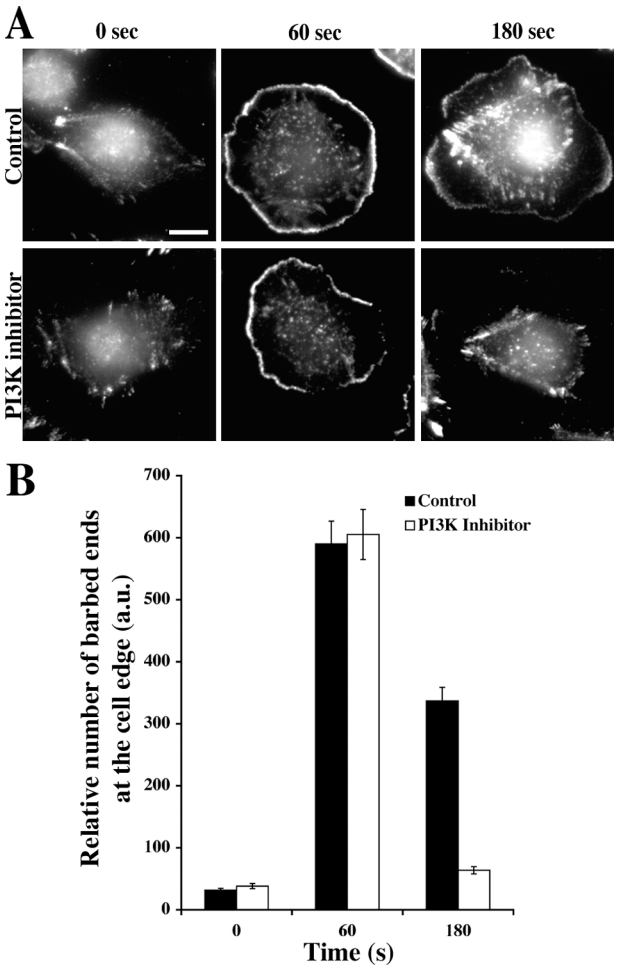

Figure 4. **PI3K inhibition selectively suppresses the generation of free barbed ends during the late transient.** (A) Representative images of the barbed end assay of control cells (DMSO) and of PI3K-inhibited cells (wortmannin) at 0, 60, and 180 s after stimulation. Bar, 10 μm. (B) Plot of the relative number of barbed ends (arbitrary units of fluorescence intensity) at 0–0.22 μm inside the cell edge in control (closed bar) and in PI3K-inhibited (open bar) cells. Error bars are SEM of ~50 cells, pooled from at least three independent experiments.

titated. Fig. 4 A shows that wortmannin treatment decreased the barbed end level in the nucleation zone at 3 min but not 1 min. Quantitation of the fluorescence intensity at the cell edge showed (Fig. 4 B) that wortmannin suppressed the level of barbed ends by almost sixfold (rendering it close to control levels) at 3 min. These results are consistent with previous work, in which function-blocking antibodies, raised against the P110α subunit of PI3K, when microinjected into these carcinoma cells, inhibited the generation of free barbed ends at 3 min after EGF stimulation (Hill et al., 2000). However, as shown in the current study for the first time, the number of barbed ends was not affected during the early transient as compared with controls. From these experiments, we concluded that PI3K activity is exclusively involved in the late barbed end transient.

PLC inhibition suppresses EGF-induced actin polymerization at the leading edge and delays lamellipodium extension in live cells

To further study the contribution of PLC to the EGF-induced actin polymerization and cell motility, we used a fluorescence time-lapse microscopy technique for visualizing changes in F-actin content in living cells (Lorenz et al., 2004a,b). MTLn3 cells stably expressing GFP-β-actin were

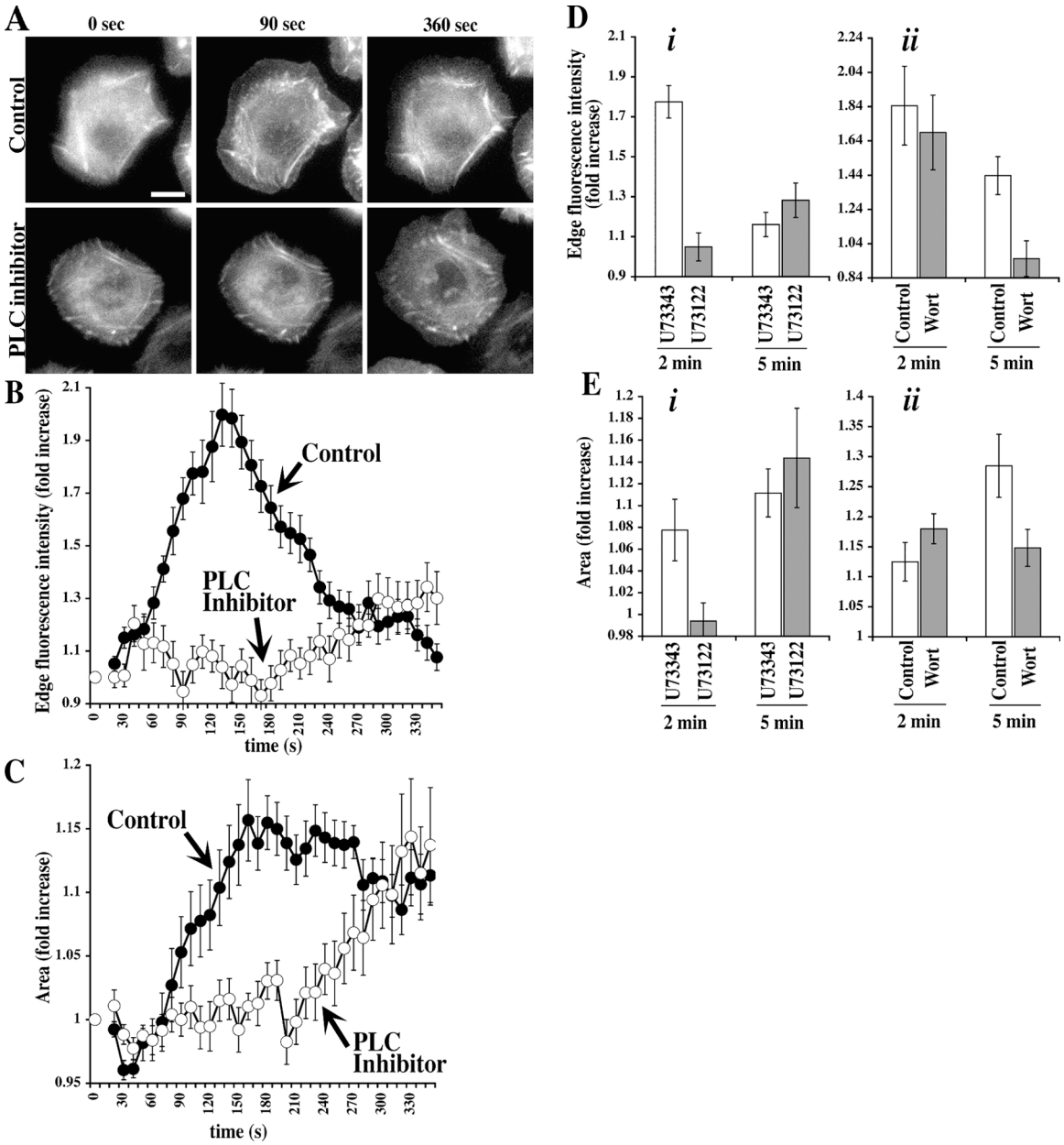

Figure 5. **PLC inhibition suppresses EGF-induced actin polymerization at the leading edge and delays lamellipodium extension.** Live-cell fluorescent microscopy of PLC-inhibited GFP-actin MTLn3 cells shows a delay in the onset of actin polymerization and membrane protrusion in response to EGF. (A) Still images (at 0, 90, and 360 s after stimulation) of two representative cells treated with the inactive (control) or the active isoform of the PLC inhibitor. Bar, 10 μm. (B) The average fold increase (over 0 s) in GFP fluorescence intensity, corresponding to F-actin, at the cell edge in control (closed circles) and in PLC-inhibited cells (open circles). (C) The average fold increase (over 0 s) in membrane protrusion (Area) of the same cells (time is in seconds after stimulation). The fold change (over 0 s) in F-actin at the cell edge (D) and in cell area (E) at 2 and 5 min in cells treated with U73343 (i, white bars), U73122 (i, gray bars), DMSO control (ii, white bars), and wortmannin (ii, gray bars) is shown. The error bars are SEM values of the averages of 15 cells, in each group, pooled from three independent experiments.

used in these experiments. This microscopy technique allowed us to quantitate both changes in F-actin levels at the leading edge and lamellipod extension in response to EGF by time-lapse, of which Fig. 5 A shows representative still pictures. This assay was used to measure the changes in F-actin levels at the leading edge (Fig. 5 B), but not free barbed ends. Inhibition of PLC activity abolished the early EGF-induced increase of F-actin (Fig. 5 B; and Fig. 5 D, i). However, F-actin levels started increasing by 200 s after EGF addition, indicating that later actin polymerization was not affected. On the contrary, inhibition of PI3K suppressed the late increase in F-actin and did not affect early F-actin levels (Fig. 5 D, ii). Similarly, analysis of lamellipodium extension revealed that inhibition of PLC halted membrane protrusion until the F-actin levels increased at 250 s after stimulation, at which lamellipod extension occurred (Fig. 5 C; and Fig. 5 E, i), and that PI3K inhibition suppressed protrusion significantly in addition to suppressing the late increase in F-actin levels (Fig. 5 D, ii; and Fig. 5 E, ii). These results revealed that PLC inhibition only de-

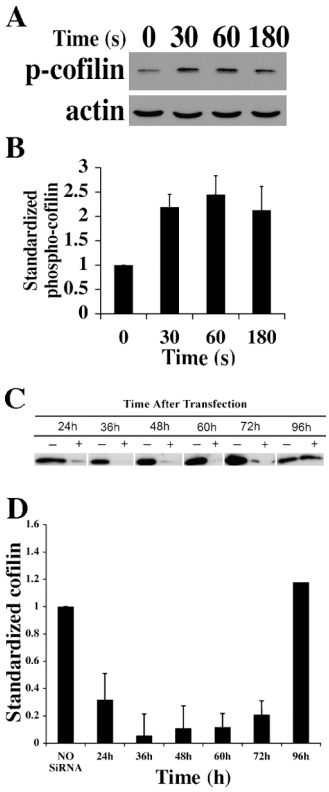

Figure 6. **EGF stimulation does not induce cofilin dephosphorylation in MTLn3 cells.** (A) Representative Western blot for p-cofilin in MTLn3 cells at 0, 30, 60, and 180 s after stimulation. (B) Plot of p-cofilin band intensities standardized over the corresponding actin bands (time is in seconds after stimulation). (C) Cofilin siRNA suppresses the levels of cofilin expression in MTLn3 cells. Representative Western blot of cofilin after cofilin RNAi transfection or after control treatment with oligofectamine (time is in hours after transfection). White lines indicate that intervening lanes have been spliced out. (D) Quantitation of anti-cofilin Western blotting analysis of lysates at different time points after transfection. Error bars are SEM of averages of at least three independent experiments.

lays the EGF-induced lamellipodium extension, whereas full lamellipod extension requires PI3K activity.

Dephosphorylation is not the major activating mechanism of cofilin in carcinoma cells

The phosphorylation status of cofilin is an important regulatory switch for cofilin activity in some cell types. For example, in resting polymorphonuclear leukocytes, the majority of cofilin is in the phosphorylated state, whereas chemoattractant stimulation causes a large dephosphorylation and activation of cofilin (Zhan et al., 2003).

However, previous work has shown that resting carcinoma cells contain lower levels of phospho-cofilin (Zebda et al., 2000). Therefore, we determined the effect of EGF stimulation on phospho-cofilin levels in carcinoma cells and found that the level of phospho-cofilin increases after EGF stimulation (Fig. 6, A and B). This finding suggests that cofilin activity is unlikely to be regulated by dephosphorylation in MTLn3 cells, which is consistent with the hypothesis that PLC hydrolysis of PIP2 in response to EGF, independent of cofilin dephosphorylation, could be the major pathway for cofilin activation.

Suppression of cofilin activity selectively inhibits the early barbed end transient

Previous work from our group has shown that the actin-severing activity of cofilin is important for the generation of free barbed ends at the leading edge in response to EGF (Chan et al., 2000; Ichetovkin et al., 2000). In vitro studies demonstrated that PIP2 regulates cofilin activity by binding cofilin and inhibiting cofilin from binding to F-actin (Yonezawa et al., 1990). Therefore, we suspected that PLC activity might be responsible for the EGF-induced cofilin activation through PIP2 hydrolysis. This model predicts that the suppression of cofilin expression would have an effect on the actin polymerization transients similar to that observed when PLC is inhibited. We used cofilin-specific small interfering RNA (siRNA) to knock down cofilin expression in MTLn3 cells. Western blot analysis was performed on cell lysates from different time points after transfection with the double-stranded siRNA (from 0 to 96 h) to monitor the cofilin levels in those cells (Fig. 6 C). Quantitation of the cofilin immunoblot bands revealed that the cofilin expression in the siRNA-transfected cultures is suppressed almost 95% 36 h after transfection, but then returns to baseline by 96 h (Fig. 6 D).

The cofilin siRNA specifically targets the cofilin message, for the sequence of the oligonucleotides used is exclusively present in the cofilin mRNA and not in that of ADF. However, the anti-cofilin antibody used in the Western blot analysis is a polyclonal antibody against the full-length cofilin protein. Due to the presence of conserved domains between cofilin and ADF, this antibody recognizes epitopes in the ADF protein as well, which runs on gels at approximately the same molecular weight as cofilin. If there were compensation by an increase in ADF expression level in the cofilin knockdown cells, this increase would have been detected in the Western blot (Fig. 6 C). Therefore, the Western blot analysis presented in Fig. 6 (C and D) indicates that the cofilin silencing decreases the antibody reactive band for cofilin by at least 95%, suggesting that ADF is a minor isoform and is not expressed at higher levels in siRNA-treated cells.

We used the barbed end assay to examine the effect of cofilin siRNA on the EGF-induced generation of free barbed ends. Cells were transfected with cofilin siRNA, or similarly treated with oligofectamine (control), and then the assay was performed at 36 h after transfection. The knock down of cofilin selectively suppressed the early barbed end transient but did not affect the late transient (Fig. 7, A and B).

The same experiment was repeated using cofilin function-blocking antibodies. The antibody was injected at saturating concentrations, previously established to totally suppress the activity of cofilin in MTLn3 cells (DesMarais et al., 2004; Lorenz et al., 2004a), and mouse IgG was injected in parallel samples as control. The cofilin function-blocking antibody injection selectively suppressed the generation of free barbed ends during the early transient but not the late transient (Fig. 7, C and D).

These results indicate that cofilin activity is involved in the early actin polymerization transient (but not the late) and supports the model that PLC regulates the early barbed end transient through its regulation of cofilin activity.

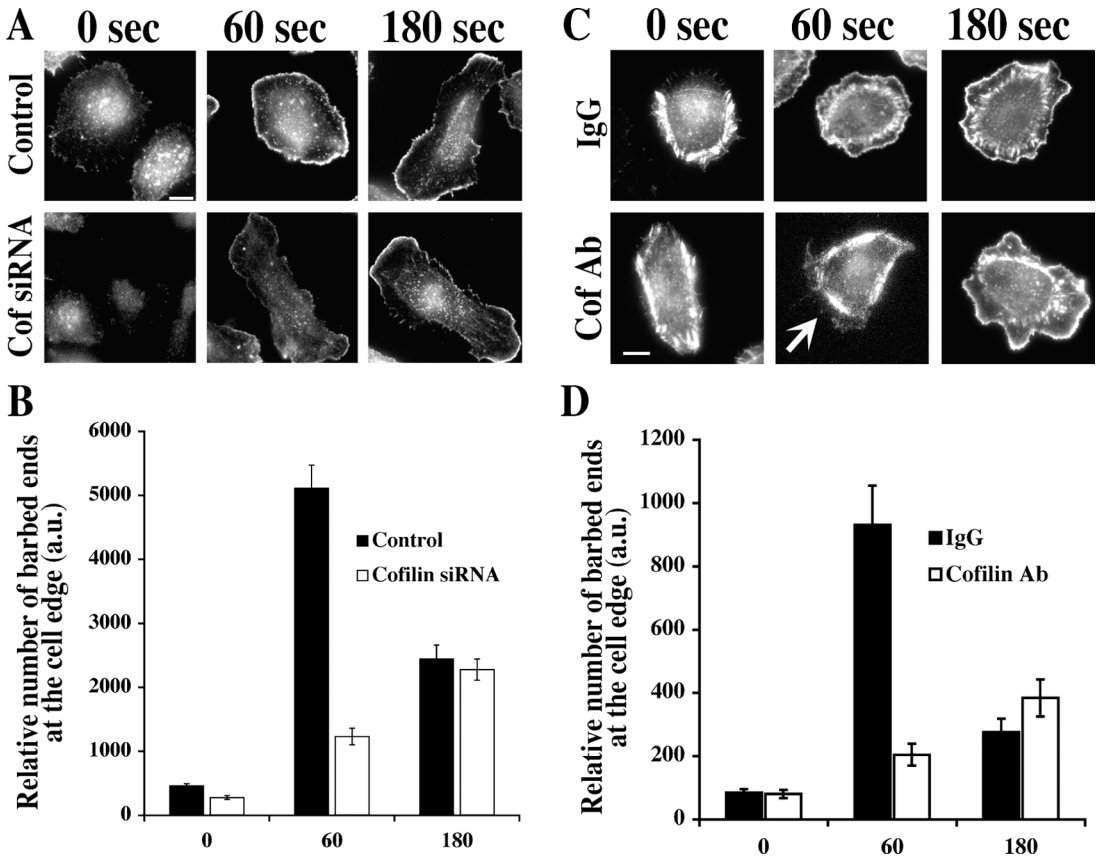

Figure 7. **Suppression of cofilin expression, or blocking cofilin function, selectively inhibits the early (but not the late) barbed end transient.** (A) Representative images of the barbed end assay (performed at 36 h after transfection) of control (oligofectamine) and of cofilin siRNA-transfected cells at 0, 60, and 180 s after stimulation. (C) Representative images of the barbed end assay of IgG and of cofilin function-blocking antibody-injected cells at 0, 60, and 180 s after stimulation (arrow indicates the limits of the cell edge as traced in phase contrast). Bars, 10 μm. (B and D) Relative number of barbed ends (closed bars represent control cells and open bars cofilin knockdown cells in B and cofilin Ab-injected cells in D) at 0–0.22 μm inside the cell edge versus time after stimulation. Error bars are SEM of ~50 cells, pooled from at least three independent experiments.

PLC inhibition suppresses the EGF-induced cofilin severing activity in MTLn3 cells

To test the hypothesis that PLC regulates actin polymerization by regulating cofilin activity, we measured cofilin activity in MTLn3 cell lysates prepared from cells after EGF stimulation with or without inhibition of PLC. We used a modified version of a light microscope severing assay (Chan et al., 2000; Ichetovkin et al., 2000). We previously demonstrated, using this assay, that the severing activity of cofilin increases in MTLn3 cells at 1 min after EGF stimulation (Chan et al., 2000). Using this assay, EGF stimulation was observed to induce an increase in cofilin activity at 1 min, which then dropped to nonstimulated levels at 3 min (Fig. 8). This increase was completely inhibited by cofilin function-blocking antibodies (unpublished data), indicating that severing is due to cofilin activity.

Inhibition of PLC activity with U73122 suppressed the cofilin activity observed at 1 min after EGF stimulation. The basal cofilin activity levels, observed at 0 and 3 min, did not change (Fig. 8 A). Treatment with the inactive isoform of the drug U73343 had no effect on cofilin activity (Fig. 8 A), which remained similar to DMSO control levels at all time points. Moreover, inhibition of PI3K activity did not have an effect on the cofilin activity profile (Fig. 8 B). These results confirm that PLC activity is necessary for inducing cofilin severing activity during the early barbed end transient, whereas PI3K is not, and indicates that the PLC-dependent free barbed end generation observed during the early transient is dependent on cofilin activity.

PLC activity determines the orientation of cell movement during chemotaxis

To determine the involvement of the PLC-dependent early polymerization transient in chemotaxis, in carcinoma cells, we used a micropipette chemotaxis assay. An EGF-filled pipette was placed in the proximity of quiescent cells, and membrane protrusion was monitored in time-lapse. Control cells, either untreated (not depicted) or treated with the inactive isoform of the PLC inhibitor (Fig. 9 A), showed an immediate and oriented protrusion toward the pipette (Fig. 9 B). The protrusion toward the pipette was defined as the "front protrusion," which started almost directly after the introduction of the pipette and continued progressing after the pipette was removed (90 s later) until it reached a plateau in 5 min (Fig. 9 B). The kinetics and extent of the front protrusion is similar to those observed in the global EGF upshift experiments (Fig. 5). In contrast, the back and the side of the control cells (the sides not facing the pipette), did not

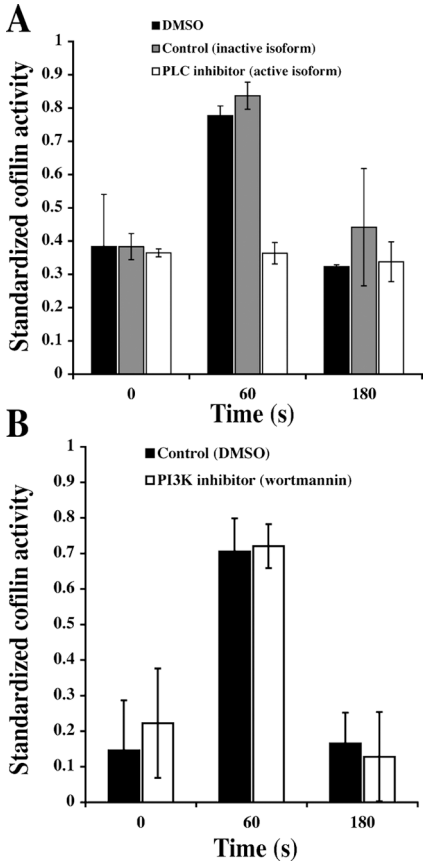

Figure 8. **PLC inhibition (but not PI3K inhibition) selectively suppresses cofilin activity at 1 min after stimulation.** (A) Cofilin activity in DMSO- (black bars), U73343- (gray bars), and U73122 (white bars)-treated cells at 0, 60, and 180 s after stimulation. (B) Cofilin activity in DMSO- (black bars) and wortmannin (white bars)-treated cells at 0, 60, and 180 s after stimulation. Cofilin activity was standardized over total protein content. Errors bars are SEM of the averages of three independent experiments.

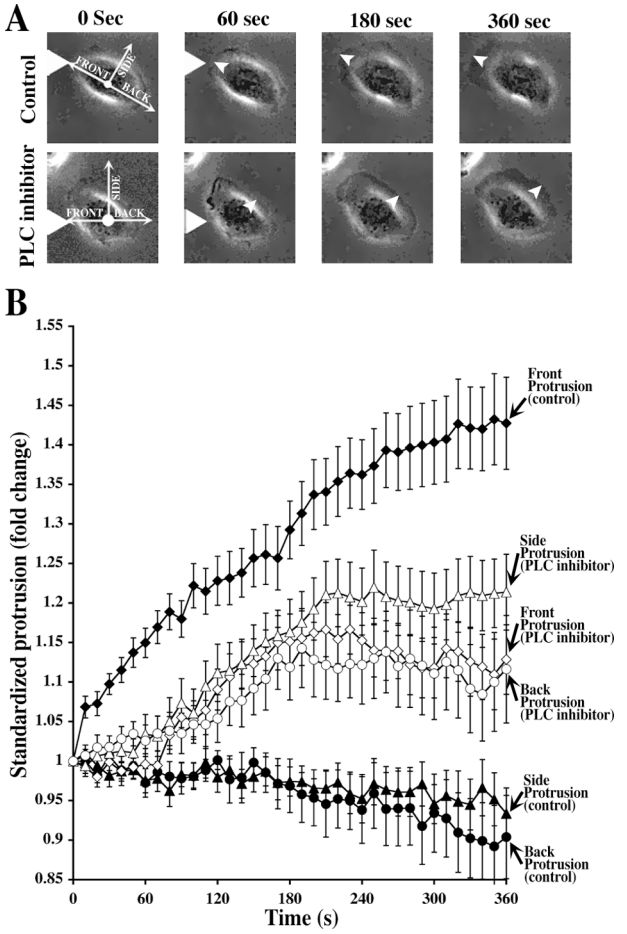

Figure 9. **PLC activity is required for directional protrusion in response to an EGF source.** (A) The response of a control (U73343) cell (top) and of a PLC-inhibited (U73122) cell (bottom) to an EGF microneedle (the white triangle represents the position of the tip of the needle, and the white arrowhead indicates the direction of protrusion). (B) The quantitation of membrane protrusion at: (a) the front of cells (corresponding to the protrusion along the front axis formed between the cell centroid and the tip of the pipette), closed diamonds represent control and open diamonds PLC-inhibited cells; (b) the side of cells (corresponding to the axis that forms a 90° angle with the front axis), closed triangles represent control and open triangles PLC-inhibited cells; (c) the back of cells (corresponding to the axis that forms a 180° angle with the front axis), closed circles represent control and open circles PLC-inhibited cells. Error bars are SEM values of the averages of 15 cells, in each group, pooled from at least three independent experiments.

show any protrusion (Fig. 9 B), and retraction was observed ~10 min after stimulation (not depicted), corresponding to polarization and onward movement of the cell toward the original position of the pipette.

PLC inhibition with U73122 affected the orientation and localization of the protrusion. The front, side, and back regions of the PLC-inhibited cells protruded to the same extent as each other, with delayed kinetics similar to the effect observed in Fig. 5 (Fig. 9, A and B). However, inhibition of PLC activity did not decrease the final extent of membrane protrusion (total area increase), where the area of PLC-inhibited cells increased 1.23 ± 0.04-fold and the area of control cells increased 1.24 ± 0.06-fold at 6 min after stimulation with the pipette. From this result, we conclude that PLC activity is required for protrusion formation toward a source of EGF.

Discussion

The motility cycle in chemotactic cells requires an initiating signal in the form of a chemoattractant. The chemoattractant results in actin polymerization at the future leading edge of the cell. Filament elongation due to polymerization pushes the membrane outward to form a protrusion completing the first step of the motility cycle (Lauffenburger and Horwitz, 1996; Bailly et al., 2001). The first protrusion determines the direction of subsequent cell locomotion. Therefore, where actin polymerization occurs first determines cell direction.

Chemotactic cells exhibit early and late transients of free barbed ends in response to a single chemoattractant stimulus. The early barbed end transient may contribute to the initial asymmetry during chemotaxis. In this work, we have investigated this early transient.

We found that the early transient of barbed ends is cotemporal with peaks of PLC and cofilin activities, and that both PLC and cofilin activities are required for the early but not the late transient of barbed ends. Furthermore, we found that the activity of cofilin during the early transient requires

PLC activity, suggesting that PLC is regulating the early barbed end transient through cofilin. These results also suggest that the early cofilin-dependent transient might be responsible for the connection between PLC activity and EGF-stimulated cell motility (Chou et al., 2003).

Inhibition of PI3K activity suppresses the late but not the early transient of free barbed ends. This finding implies that the early and the late actin polymerization transients are differentially regulated by two signaling pathways, a PLC-dependent one and a PI3K-dependent one, respectively.

Despite PLC inhibition, lamellipodium extension still occurs, but is delayed until actin polymerization increases, concomitantly with the late transient of barbed ends. Moreover, inhibition of PLC abolishes the directional sensing and protrusion observed in response to an EGF gradient. Although the size of the EGF-induced protrusion is not affected, its location and the subsequent orientation of the cell locomotion toward the EGF source fails to occur in PLC-inhibited cells.

These results suggest that PLC-dependent activation of cofilin could determine the initial asymmetric polymerization of actin (the early transient) to cause protrusion toward the source of EGF. This is consistent with the ability of localized activation of cofilin to determine the location of protrusion and cell direction in uncaging experiments (Ghosh et al., 2004).

The late transient of barbed ends and its coupled lamellipod extension are abolished when PI3K is inhibited with either a function-blocking antibody as shown previously (Hill et al., 2000) or with wortmannin as in our study. This suggests that, during locomotion, the late PI3K-dependent transient of free barbed ends is more implicated in lamellipodium extension than the early cofilin-dependent one.

The participation of PLC in EGF-induced actin polymerization

Cofilin can be phosphorylated on Ser 3 by LIM-kinase, and this inhibits its actin-binding activity. LIM-kinase has been shown to phosphorylate cofilin, and this was correlated with increased stability of F-actin in cells at equilibrium (Arber et al., 1998) and loss of barbed ends and protrusion activity in response to EGF (Chan et al., 2000; Zebda et al., 2000).

In some resting cells, cofilin is mostly phosphorylated (Moriyama et al., 1996). Stimulation of motility by a variety of agents induces dephosphorylation and activation of cofilin (Kanamori et al., 1995; Okada et al., 1996). In neutrophils, cofilin dephosphorylation was shown to be dependent on PLC activity (Zhan et al., 2003). However, in insulin-stimulated fibroblasts dephosphorylation of cofilin, which was also shown to be the major mechanism of cofilin activation, is PI3K dependent (Nishita et al., 2003). This finding shows that the mechanism and the time of cofilin dephosphorylation are not conserved among cell types.

In carcinoma cells, at least half of cofilin is in the dephosphorylated state, yet cofilin is inactive (Chan et al., 2000; Zebda et al., 2000). Furthermore, cofilin is phosphorylated upon EGF stimulation, indicating a more complex regulatory mechanism than simply dephosphorylation of cofilin. Hence, the PLC-induced dephosphorylation of cofilin, observed in neutrophils (Zhan et al., 2003), is unlikely to be the main regulatory pathway to cofilin activation in carcinoma cells. Because the actin-binding activity of cofilin is regulated in vitro by PIP2 binding (Yonezawa et al., 1991), in addition to LIM-kinase–dependent phosphorylation, the dephosphorylated cofilin may be kept inactive by binding to PIP2 in resting cells.

This hypothesis is supported by several observations: (a) EGF stimulation induces PLC activity in MTLn3 cells, leading to the hydrolysis of PIP2 and this is correlated with a decrease in the colocalization of PIP2 and cofilin by immunofluorescence at the plasma membrane upon EGF stimulation (unpublished data). (b) Previous studies have shown that artificially increasing PIP2 levels leads to an increase in steady-state actin filaments (Sakisaka et al., 1997; Shibasaki et al., 1997; Rozelle et al., 2000; Yamamoto et al., 2001). This phenotype is consistent with that observed for cofilin inactivation (Zebda et al., 2000), supporting a model where cofilin's depolymerizing activity is inhibited by PIP2. (c) Activated (p-Tyr) PLCγ1 can hydrolyse PIP2 that is bound to profilin leading to its release and activation (Goldschmidt-Clermont et al., 1991). A similar mechanism may be at work to release cofilin from PIP2 upon EGF stimulation of carcinoma cells.

Other actin-binding proteins are also regulated by PIP2. Capping protein may be dissociated from the membrane when PIP2 levels drop after PLC activation. Capping protein binds and caps the free barbed ends of actin filaments, hence reducing the number of nucleation sites. The reconstitution of PIP2 levels at the membrane could lead to the uncapping of the filament ends (Cooper and Schafer, 2000). Thus, the increase in PLC activity may counteract the generation of free barbed ends by capping protein and may limit the extent of new filament growth after stimulation (Eddy et al., 1996). NWASP can be stimulated by PIP2 to interact with the Arp2/3 complex, and PIP2 contributes to the recruitment of the NWASP to the membrane (Takenawa and Miki, 2001). However, Grb2 and Nck were also shown to activate NWASP and contribute to the membrane recruitment (Takenawa and Miki, 2001). Therefore, a drop in PIP2 levels could still occur concomitantly with an increase in NWASP activity and membrane recruitment, which is consistent with NWASP activation and membrane recruitment during the PLC activation transient in MTLn3 cells (Lorenz et al., 2004b; Sukumvanich et al., 2004).

Interaction between the PLC and the PI3K pathways in generating barbed ends

PI3K has been postulated to regulate actin polymerization through the activation of the Arp2/3 complex. PI3K activates WASP family proteins via the activation of small GTPases, and WASP proteins are known to be the main activators of the Arp2/3 complex (Higgs and Pollard, 2001; Takenawa and Miki, 2001). Analysis of the effects of the function-blocking antibody against p34 that inhibits Arp2/3 complex function demonstrates that Arp2/3 activity is required for the production of barbed ends in MTLn3 cells (DesMarais et al., 2004).

In carcinoma cells, cofilin severing activity and Arp2/3-branching activity cooperate in lamellipod extension (DesMarais et al., 2004). This synergy between the two effectors is explained in vitro by the preference of the Arp2/3 complex for newly polymerized filaments generated by cofilin severing (Ichetovkin et al., 2002). This synergy has been pro-

posed as the mechanism by which pushing force, leading to membrane protrusion, is generated at specific sites on the cell surface (DesMarais et al., 2004). This model predicts that the local activation of cofilin will define the site of protrusion and subsequent cell direction, which has been observed using caged cofilin (Ghosh et al., 2004). This model also predicts that inhibition of cofilin activity will delay the generation of both the barbed ends and protrusive force, and this was observed in our work.

In conclusion, we have defined two distinctly regulated actin polymerization transients essential for the initiation and progression of carcinoma cell chemotaxis. The first transient is PLC and cofilin-dependent and it demarcates the position of the future leading edge on the cell membrane, hence setting the initial asymmetry in response to a gradient of EGF. The second transient is PI3K and Arp2/3 complex dependent and it generates most of the protrusive force leading to lamellipod extension and prefers to act at sites where cofilin is active. Together, these activities initiate the cell motility cycle, after EGF stimulation, and are required for chemotaxis to EGF.

Materials and methods

Cell culture

MTLn3 cells (rat mammary adenocarcinoma cell line) were maintained, starved, and stimulated as described previously (DesMarais et al., 2004). For light microscopy experiments, cells were plated on glass bottom dishes (MatTek Corporation), which had been treated with 1 M HCl for 10 min, followed by one wash with 75% ethanol, and then one wash with PBS. Before each experiment, cells were starved in L15 medium (GIBCO BRL) supplemented with 0.35% BSA (starvation medium) for 3 to 4 h. For stimulation, MTLn3 cells were treated at 37°C with a bath application of 5 nM EGF (Invitrogen) for various times, except for the pipette assay where EGF was introduced in a pipette (see The micropipette assay).

Antibodies and inhibitors

The Cy5-conjugated antibiotin was obtained from Jackson ImmunoResearch Laboratories; the anti-PLCγ1 was obtained from Upstate Biotechnology; U73122 and U73343 were obtained from BIOMOL Research Laboratories, Inc.; and wortmannin was obtained from Sigma-Aldrich. U73122 and U73343 were used at 5 μM in starvation medium. Wortmannin was used at 100 nM in BSA-free starvation medium.

Light microscopy and quantitation

All pictures (except for the pipette assay—see The micropipette assay) were taken using a 60 × NA 1.4 infinity-corrected optics on a microscope (model IX170; Olympus) supplemented with a computer-driven cooled CCD camera and operated by IPLab Spectrum software (VayTek). Digital images were linearly converted in NIH image and analyzed using macro analysis. In brief, the software averages the fluorescence intensity in 29 annuli, ranging from 1.1 μm outside the cell periphery and extending to the same distance inside the cell (consecutive annuli are 0.22 μm apart from each other).

Cofilin siRNA

The cofilin siRNA duplexes were designed against the following *cofilin* gene sequence: 5′ AAGGTGTTCAATGACATGAAA 3′. MTLn3 cells were transfected with the cofilin siRNA duplex in the presence of oligofectamine (Invitrogen). The transfection was terminated after 4 h by using 2× serum containing media. Control experiments for the use of this siRNA duplex were the rescuing of the inhibition of barbed ends caused by this siRNA by uncaging cofilin (Ghosh et al., 2004) and the use of function-blocking antibodies against cofilin, which reproduced the same phenotype (Fig. 7).

Barbed end assay and microinjection

To measure the number of free barbed ends in response to EGF and to stain for F-actin with rhodamine-phalloidin, we used a previously described assay (Chan et al., 1998), which we denote as the barbed end assay. Quantitation of fluorescence intensity (see Light microscopy and quantitation) versus distance from the cell periphery was used to determine the number of free barbed ends in the leading edge (Fig. 1 B). The average intensities, which correspond to the zone between 0 and 0.22 μm inside the cell (shaded area in Fig. 1 B), plotted separately versus time reveal that the generation of free barbed ends in response to EGF stimulation follows two transients with the two peaks corresponding to 1 and 3 min after addition of EGF (Fig. 1 C). Microinjection of the cofilin function-blocking antibody was performed as described previously (DesMarais et al., 2004).

Live-cell imaging

GFP-actin expressing MTLn3 cells were used as described previously (Lorenz et al., 2004a). In brief, time-lapse series of the cells after EGF stimulation were taken using a 60× NA 1.4 infinity-corrected optics on a microscope and analyzed in NIH image using macro analysis (see Light microscopy and quantitation). Chemotactic cells exhibit early and late transients of free barbed ends in response to a single chemoattractant stimulus, as observed in the barbed end assay (Fig. 1). However, the increase in F-actin at the leading edge follows different kinetics (examined using the GFP-actin live-cell imaging), corresponding to the sum of polymerization and depolymerization of actin at the leading edge (Fig. 5). Therefore, the barbed end assay and the GFP-actin imaging assay measure two different parameters, the availability of actin nucleation sites and the accumulation of total F-actin at the leading edge, respectively.

Immunoblotting

After EGF stimulation for various time points, cells were promptly rinsed with cold PBS supplemented with 0.018 mg/ml $NaVO_4$ and lysed with warm 2× sample buffer. The samples were subjected to SDS-PAGE followed by Western blotting.

Cofilin severing activity assay

The relative cofilin severing activity in MTLn3 cell lysates was quantitated using a modified version of the previously established light microscopy severing assay (Ichetovkin et al., 2000). Rhodamine- and biotin-actin filaments (on beads) were incubated with cell lysates for 10 min at RT. Total fluorescence was quantitated in ImageJ, and relative cofilin activity was measured as the decrease in fluorescence after adding the lysates: relative cofilin activity = [(fluorescence intensity after adding lysis buffer alone) − (fluorescence intensity after adding cell lysates)] / (fluorescence intensity after adding lysis buffer alone). All the relative cofilin activity measurements were standardized over the total protein content.

The micropipette assay

A Femtojet Micromanipulator 5171 (Eppendorf-Brinkman Instruments) and a pump, (model Femtojet; Eppendorf) were used to control the position of the micropipette and the pressure required for the chemoattractant flow. U73122 was used to inhibit PLC, and U73343 was used as a control. To induce the formation of protrusion, a micropipette was filled with 25 nM EGF and was placed ∼5 μm from the edge of a quiescent cell, and a pressure of 16 hPa was exerted to induce flow. Time-lapse series were taken using 20× NA 1.4 infinity-corrected optics on a microscope and analyzed in ImageJ. Protrusion is measured along three lines emanating from the cell centroid: (1) the front protrusion is measured along the axis formed by the centroid and the tip of the pipette; (2) the side protrusion is measured along the perpendicular to the latter; and (3) the back protrusion is measured along the axis forming 180° with the front axis. All measurements are standardized over the corresponding distance between the centroid and the cell periphery along the corresponding axis before the introduction of the pipette.

We are grateful to the Analytical Imaging Facility at Albert Einstein College of Medicine, especially to Michael Cammer for his valuable assistance in image analysis.

This work was supported by National Institutes of Health grants GM38511 (J. Condeelis) and CA100324 (J. Backer).

Submitted: 26 May 2004
Accepted: 16 July 2004

References

Abercrombie, M., J.E. Heaysman, and S.M. Pegrum. 1972. Locomotion of fibroblasts in culture. V. Surface marking with concanavalin A. *Exp. Cell Res.* 73:536–539.

Allen, P.G. 2003. Actin filament uncapping localizes to ruffling lamellae and rocketing vesicles. *Nat. Cell Biol.* 5:972–979.

Arber, S., F.A. Barbayannis, H. Hanser, C. Schneider, C.A. Stanyon, O. Bernard, and P. Caroni. 1998. Regulation of actin dynamics through phosphorylation

of cofilin by LIM-kinase. *Nature.* 393:805–809.

Bailly, M., and J. Condeelis. 2002. Cell motility: insights from the backstage. *Nat. Cell Biol.* 4:E292–E294.

Bailly, M., I. Ichetovkin, W. Grant, N. Zebda, L.M. Machesky, J.E. Segall, and J. Condeelis. 2001. The F-actin side binding activity of the Arp2/3 complex is essential for actin nucleation and lamellipod extension. *Curr. Biol.* 11:620–625.

Bleasdale, J.E., G.L. Bundy, S. Bunting, F.A. Fitzpatrick, R.M. Huff, F.F. Sun, and J.E. Pike. 1989. Inhibition of phospholipase C dependent processes by U-73, 122. *Adv. Prostaglandin Thromboxane Leukot. Res.* 19:590–593.

Chan, A.Y., S. Raft, M. Bailly, J.B. Wyckoff, J.E. Segall, and J.S. Condeelis. 1998. EGF stimulates an increase in actin nucleation and filament number at the leading edge of the lamellipod in mammary adenocarcinoma cells. *J. Cell Sci.* 111:199–211.

Chan, A.Y., M. Bailly, N. Zebda, J.E. Segall, and J.S. Condeelis. 2000. Role of cofilin in epidermal growth factor–stimulated actin polymerization and lamellipod protrusion. *J. Cell Biol.* 148:531–542.

Chen, L., C. Janetopoulos, Y.E. Huang, M. Iijima, J. Borleis, and P.N. Devreotes. 2003. Two phases of actin polymerization display different dependencies on PI(3,4,5)P3 accumulation and have unique roles during chemotaxis. *Mol Biol Cell.* 14:5028–5037.

Chen, P., K. Gupta, and A. Wells. 1994. Cell movement elicited by epidermal growth factor receptor requires kinase and autophosphorylation but is separable from mitogenesis. *J. Cell Biol.* 124:547–555.

Chou, J., N.A. Burke, A. Iwabu, S.C. Watkins, and A. Wells. 2003. Directional motility induced by epidermal growth factor requires Cdc42. *Exp. Cell Res.* 287:47–56.

Comer, F.I., and C.A. Parent. 2002. PI 3-kinases and PTEN: how opposites chemoattract. *Cell.* 109:541–544.

Cooper, J.A., and D.A. Schafer. 2000. Control of actin assembly and disassembly at filament ends. *Curr. Opin. Cell Biol.* 12:97–103.

Cox, D., J. Condeelis, D. Wessels, D. Soll, H. Kern, and D.A. Knecht. 1992. Targeted disruption of the ABP-120 gene leads to cells with altered motility. *J. Cell Biol.* 116:943–955.

den Hartigh, J.C., P.M. van Bergen en Henegouwen, A.J. Verkleij, and J. Boonstra. 1992. The EGF receptor is an actin-binding protein. *J Cell Biol*. 119: 349–355.

DesMarais, V., F. Macaluso, J. Condeelis, and M. Bailly. 2004. Synergistic interaction between the Arp2/3 complex and cofilin drives stimulated lamellipod extension. *J. Cell Sci.* 117:3499–3510.

Devreotes, P., and C. Janetopoulos. 2003. Eukaryotic chemotaxis: distinctions between directional sensing and polarization. *J. Biol. Chem.* 278:20445–20448.

dos Remedios, C.G., D. Chhabra, M. Kekic, I.V. Dedova, M. Tsubakihara, D.A. Berry, and N.J. Nosworthy. 2003. Actin binding proteins: regulation of cytoskeletal microfilaments. *Physiol. Rev.* 83:433–473.

Eddy, R.J., J. Han, R.A. Sauterer, and J.S. Condeelis. 1996. A major agonist-regulated capping activity in *Dictyostelium* is due to the capping protein, cap32/34. *Biochim. Biophys. Acta.* 1314:247–259.

Eddy, R.J., J. Han, and J.S. Condeelis. 1997. Capping protein terminates but does not initiate chemoattractant-induced actin assembly in *Dictyostelium*. *J. Cell Biol.* 139:1243–1253.

Falasca, M., S.K. Logan, V.P. Lehto, G. Baccante, M.A. Lemmon, and J. Schlessinger. 1998. Activation of phospholipase C γ by PI 3-kinase-induced PH domain-mediated membrane targeting. *EMBO J.* 17:414–422.

Funamoto, S., R. Meili, S. Lee, L. Parry, and R.A. Firtel. 2002. Spatial and temporal regulation of 3-phosphoinositides by PI 3-kinase and PTEN mediates chemotaxis. *Cell.* 109:611–623.

Ghosh, M., X. Song, G. Mouneimne, M. Sidani, D.S. Lawrence, and J.S. Condeelis. 2004. Cofilin promotes actin polymerization and defines the direction of cell motility. *Science.* 304:743–746.

Goldschmidt-Clermont, P.J., J.W. Kim, L.M. Machesky, S.G. Rhee, and T.D. Pollard. 1991. Regulation of phospholipase C-γ 1 by profilin and tyrosine phosphorylation. *Science.* 251:1231–1233.

Hall, A.L., V. Warren, S. Dharmawardhane, and J. Condeelis. 1989. Identification of actin nucleation activity and polymerization inhibitor in ameboid cells: their regulation by chemotactic stimulation. *J. Cell Biol.* 109:2207–2213.

Higgs, H.N., and T.D. Pollard. 2001. Regulation of actin filament network formation through ARP2/3 complex: activation by a diverse array of proteins. *Annu. Rev. Biochem.* 70:649–676.

Hill, K., S. Welti, J. Yu, J.T. Murray, S.C. Yip, J.S. Condeelis, J.E. Segall, and J.M. Backer. 2000. Specific requirement for the p85-p110α phosphatidylinositol 3-kinase during epidermal growth factor-stimulated actin nucleation in breast cancer cells. *J. Biol. Chem.* 275:3741–3744.

Ichetovkin, I., J. Han, K.M. Pang, D.A. Knecht, and J.S. Condeelis. 2000. Actin filaments are severed by both native and recombinant *dictyostelium* cofilin but to different extents. *Cell Motil. Cytoskeleton.* 45:293–306.

Ichetovkin, I., W. Grant, and J. Condeelis. 2002. Cofilin produces newly polymerized actin filaments that are preferred for dendritic nucleation by the Arp2/3 complex. *Curr. Biol.* 12:79–84.

Iijima, M., and P. Devreotes. 2002. Tumor suppressor PTEN mediates sensing of chemoattractant gradients. *Cell.* 109:599–610.

Kanamori, T., T. Hayakawa, M. Suzuki, and K. Titani. 1995. Identification of two 17-kDa rat parotid gland phosphoproteins, subjects for dephosphorylation upon β-adrenergic stimulation, as destrin- and cofilin-like proteins. *J. Biol. Chem.* 270:8061–8067.

Kassis, J., J. Moellinger, H. Lo, N.M. Greenberg, H.G. Kim, and A. Wells. 1999. A role for phospholipase C-γ-mediated signaling in tumor cell invasion. *Clin. Cancer Res.* 5:2251–2260.

Kassis, J., R. Radinsky, and A. Wells. 2002. Motility is rate-limiting for invasion of bladder carcinoma cell lines. *Int. J. Biochem. Cell Biol.* 34:762–775.

Lauffenburger, D.A., and A.F. Horwitz. 1996. Cell migration: a physically integrated molecular process. *Cell.* 84:359–369.

Lorenz, M., V. DesMarais, F. Macaluso, R.H. Singer, and J. Condeelis. 2004a. Measurement of barbed ends, actin polymerization, and motility in live carcinoma cells after growth factor stimulation. *Cell Motil. Cytoskeleton.* 57:207–217.

Lorenz, M., H. Yamaguchi, Y. Wang, R.H. Singer, and J. Condeelis. 2004b. Imaging sites of N-wasp activity in lamellipodia and invadopodia of carcinoma cells. *Curr. Biol.* 14:697–703.

Moriyama, K., K. Iida, and I. Yahara. 1996. Phosphorylation of Ser-3 of cofilin regulates its essential function on actin. *Genes Cells.* 1:73–86.

Nishita, M., Y. Wang, C. Tomizawa, A. Suzuki, R. Niwa, T. Uemura, and K. Mizuno. 2003. Phosphoinositide 3-kinase-mediated activation of cofilin phosphatase Slingshot and its role for insulin-induced membrane protrusion. *J Biol Chem*. 279:7193–7198.

Okada, K., H. Takano-Ohmuro, T. Obinata, and H. Abe. 1996. Dephosphorylation of cofilin in polymorphonuclear leukocytes derived from peripheral blood. *Exp. Cell Res.* 227:116–122.

Payrastre, B., P.M. van Bergen en Henegouwen, M. Breton, J.C. den Hartigh, M. Plantavid, A.J. Verkleij, and J. Boonstra. 1991. Phosphoinositide kinase, diacylglycerol kinase, and phospholipase C activities associated to the cytoskeleton: effect of epidermal growth factor. *J Cell Biol*. 115:121–128.

Piccolo, E., P.F. Innominato, M.A. Mariggio, T. Maffucci, S. Iacobelli, and M. Falasca. 2002. The mechanism involved in the regulation of phospholipase Cγ1 activity in cell migration. *Oncogene.* 21:6520–6529.

Raftopoulou, M., S. Etienne-Manneville, A. Self, S. Nicholls, and A. Hall. 2004. Regulation of cell migration by the C2 domain of the tumor suppressor PTEN. *Science.* 303:1179–1181.

Rebecchi, M.J., and S.N. Pentyala. 2000. Structure, function, and control of phosphoinositide-specific phospholipase C. *Physiol. Rev.* 80:1291–1335.

Rozelle, A.L., L.M. Machesky, M. Yamamoto, M.H. Driessens, R.H. Insall, M.G. Roth, K. Luby-Phelps, G. Marriott, A. Hall, and H.L. Yin. 2000. Phosphatidylinositol 4,5-bisphosphate induces actin-based movement of raft-enriched vesicles through WASP-Arp2/3. *Curr. Biol.* 10:311–320.

Sakisaka, T., T. Itoh, K. Miura, and T. Takenawa. 1997. Phosphatidylinositol 4,5-bisphosphate phosphatase regulates the rearrangement of actin filaments. *Mol. Cell. Biol.* 17:3841–3849.

Servant, G., O.D. Weiner, P. Herzmark, T. Balla, J.W. Sedat, and H.R. Bourne. 2000. Polarization of chemoattractant receptor signaling during neutrophil chemotaxis. *Science.* 287:1037–1040.

Shibasaki, Y., H. Ishihara, N. Kizuki, T. Asano, Y. Oka, and Y. Yazaki. 1997. Massive actin polymerization induced by phosphatidylinositol-4-phosphate 5-kinase in vivo. *J. Biol. Chem.* 272:7578–7581.

Sukumvanich, P., V. DesMarais, C.V. Sermiento, Y. Wang, I. Ichetovkin, C. Mouneimne, S. Almo, and J. Condeelis. 2004. Cellular localization of activated N-WASP using a conformationally sensitive antibody. *Cell Motil. Cytoskeleton.* In press.

Sun, H.Q., M. Yamamoto, M. Mejillano, and H.L. Yin. 1999. Gelsolin, a multifunctional actin regulatory protein. *J. Biol. Chem.* 274:33179–33182.

Takenawa, T., and H. Miki. 2001. WASP and WAVE family proteins: key molecules for rapid rearrangement of cortical actin filaments and cell movement. *J. Cell Sci.* 114:1801–1809.

Wu, H., V. Goel, and F.G. Haluska. 2003. PTEN signaling pathways in melanoma. *Oncogene.* 22:3113–3122.

Wyckoff, J.B., J.G. Jones, J.S. Condeelis, and J.E. Segall. 2000a. A critical step in metastasis: in vivo analysis of intravasation at the primary tumor. *Cancer Res.* 60:2504–2511.

Wyckoff, J.B., J.E. Segall, and J.S. Condeelis. 2000b. The collection of the motile population of cells from a living tumor. *Cancer Res.* 60:5401–5404.

Yamamoto, M., D.H. Hilgemann, S. Feng, H. Bito, H. Ishihara, Y. Shibasaki, and H.L. Yin. 2001. Phosphatidylinositol 4,5-bisphosphate induces actin stress-fiber formation and inhibits membrane ruffling in CV1 cells. *J. Cell Biol.* 152:867–876.

Yonezawa, N., E. Nishida, K. Iida, I. Yahara, and H. Sakai. 1990. Inhibition of the interactions of cofilin, destrin, and deoxyribonuclease I with actin by phosphoinositides. *J. Biol. Chem.* 265:8382–8386.

Yonezawa, N., Y. Homma, I. Yahara, H. Sakai, and E. Nishida. 1991. A short sequence responsible for both phosphoinositide binding and actin binding activities of cofilin. *J. Biol. Chem.* 266:17218–17221.

Zebda, N., O. Bernard, M. Bailly, S. Welti, D.S. Lawrence, and J.S. Condeelis. 2000. Phosphorylation of ADF/cofilin abolishes EGF-induced actin nucleation at the leading edge and subsequent lamellipod extension. *J. Cell Biol.* 151:1119–1128.

Zhan, Q., J.R. Bamburg, and J.A. Badwey. 2003. Products of phosphoinositide specific phospholipase C can trigger dephosphorylation of cofilin in chemoattractant stimulated neutrophils. *Cell Motil. Cytoskeleton.* 54:1–15.